Divining gold in seafloor polymetallic massive sulfide systems

Sebastian Fuchs[*]*, Mark D. Hannington and Sven Petersen*

*Corresponding author:
GEOMAR – Helmholtz Centre for Ocean Research Kiel, Wischhofstrasse 1-3, 24148 Kiel, Germany

Email: sfuchs@geomar.de

Electronic supplementary material 2

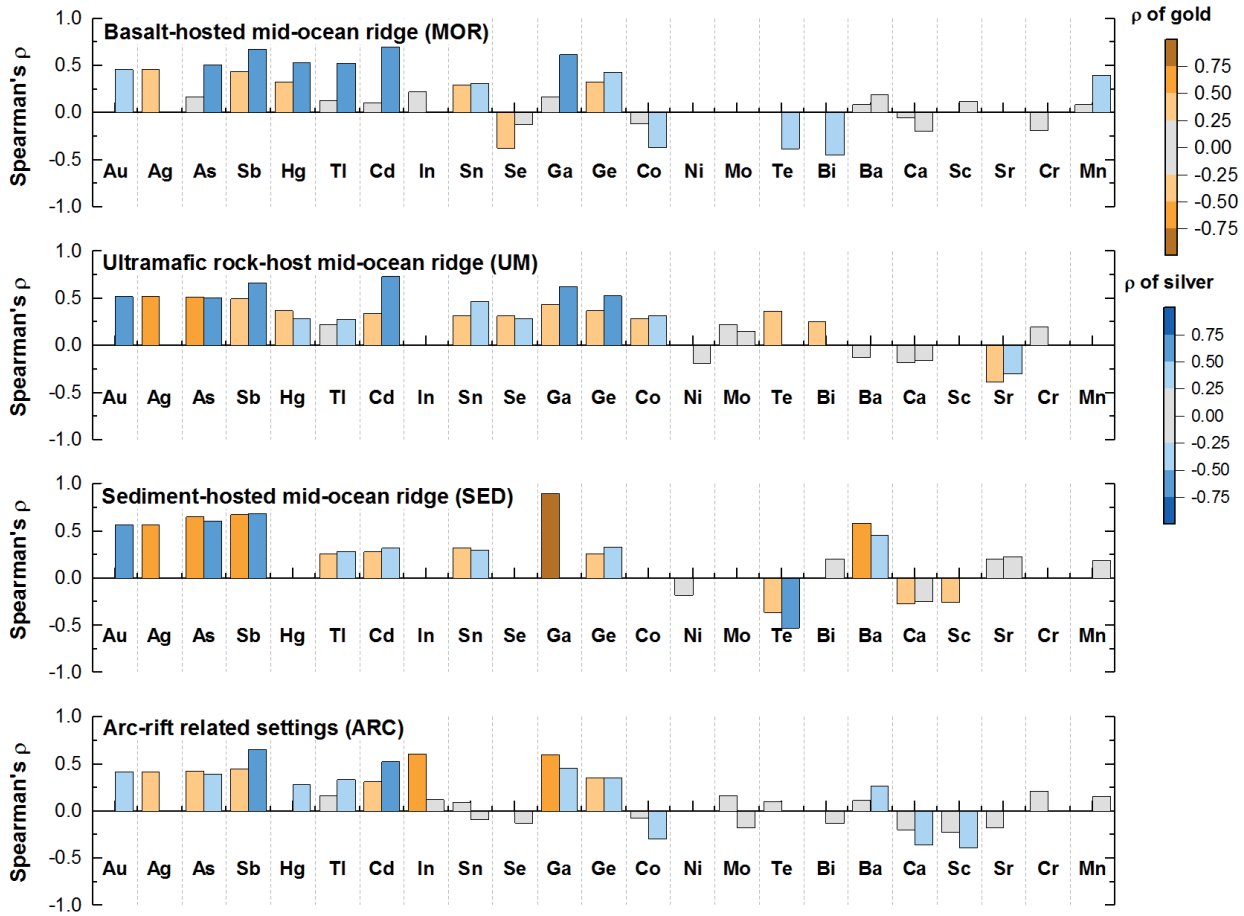

Fig. 1 (ESM 2) Histogram of Spearman's rank correlation coefficients (ρ) for trace elements versus Au (yellow) and Ag (blue) in sulfide samples from mid-ocean ridge deposits (MOR, N= 1976), ultramafic rock-hosted deposits (UM, N= 332), sediment-hosted deposits (SED, N=441), and arc-related deposits (ARC, N= 2452). The correlation coefficients for each element pair are significant at the 95% confidence level and passed a 2-tailed significance test (t-test). No bar for some trace elements indicates no significant correlation (failed t-test).

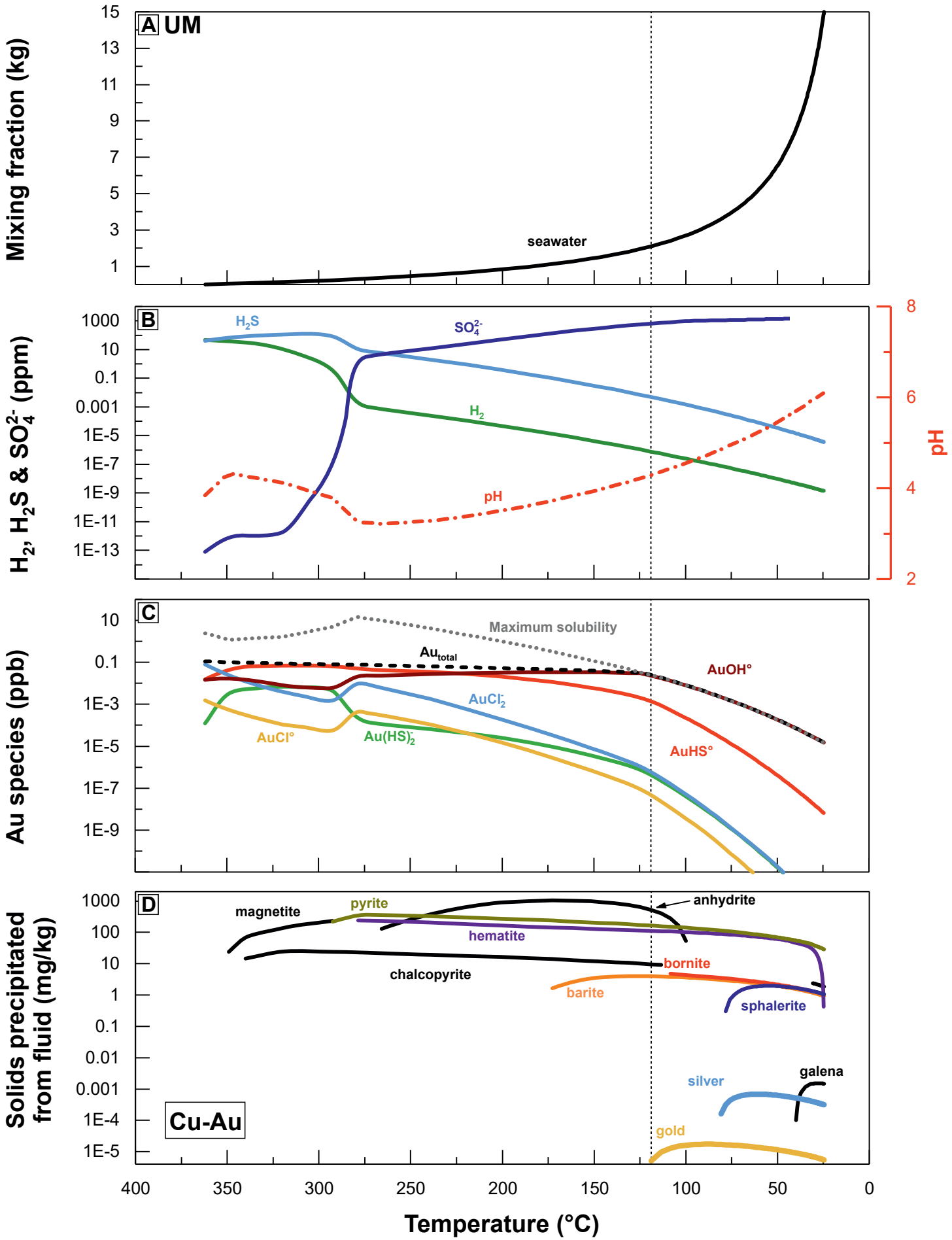

Fig. 2 (ESM 2) Geochemical reaction-path model for mixing of a typical ultramafic-hosted (UM) vent fluid with ambient seawater, using the starting composition of the Rainbow field fluid samples on the Mid-Atlantic Ridge (Table 2 in ESM 2). This model assumes incremental mixing with cold seawater (2 °C) until a final temperature 25 °C (mixing ratio 1:15). (A) shows the mixing fraction of seawater into the hydrothermal fluid. (B) shows the concentrations of aqueous H_2S, H_2 and SO_4^{2-} and the pH (right-hand axis) as a function of temperature. (C) shows the concentration of aqueous Au species. The black-dashed lines correspond to the starting concentrations of Au and Ag in the modelled fluid from Table 2 of this electronic supplementary material (ESM 2); the grey-dotted line correspond to the maximum solubility over the reaction path. (D) shows the minerals that precipitate with mixing and the resulting Cu-Au association at low temperatures. The apparent decrease in the amount of minerals precipitated at low temperature is an artifact of the increasing mass of fluid in the model as a result of mixing.

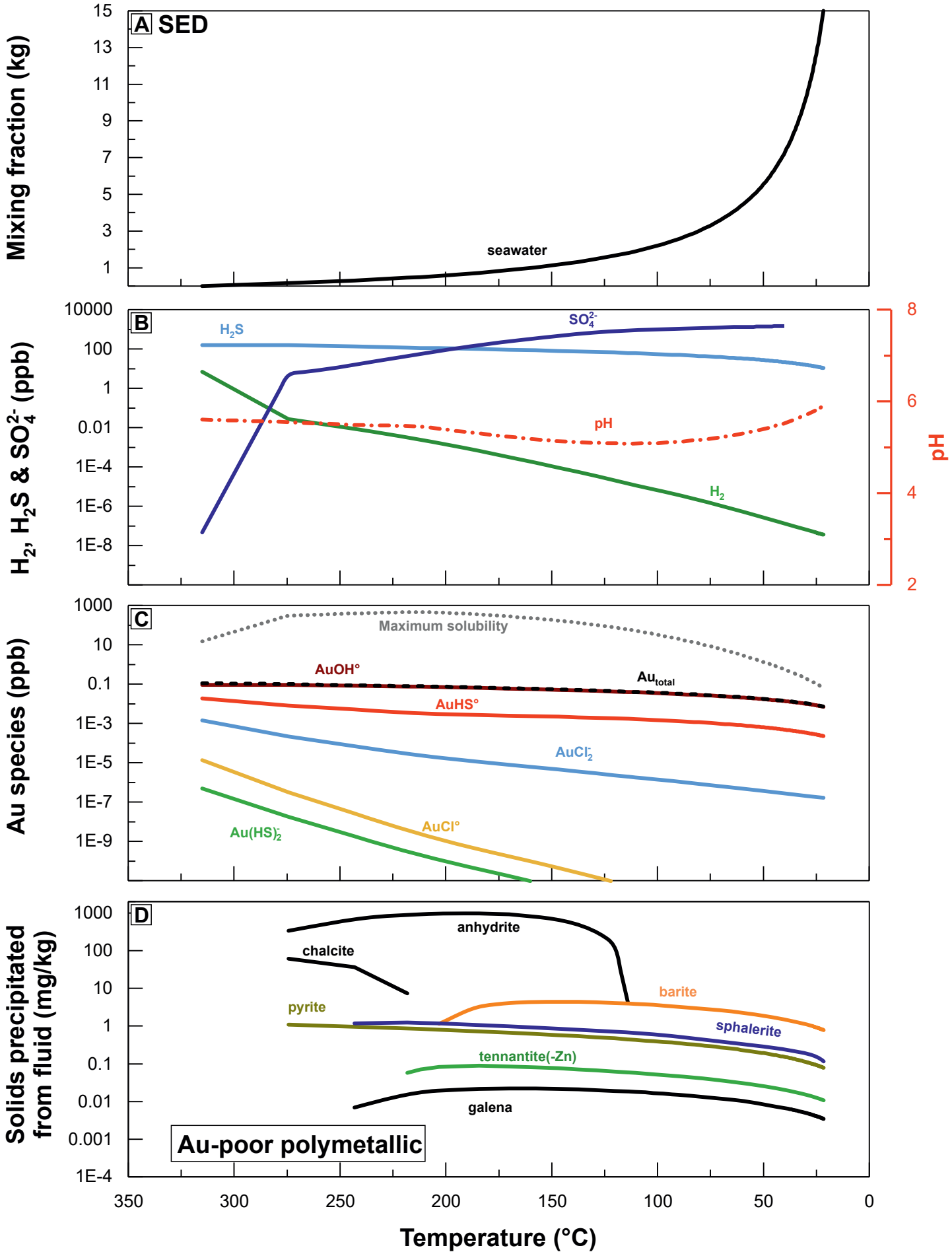

Fig. 3 (ESM 2) Geochemical reaction-path model for mixing of a typical sediment-hosted (SED) vent fluid with ambient seawater, using the starting composition of the Guaymas Basin fluid samples (Table 2 in ESM 2). This model assumes incremental mixing with cold seawater (2 °C) until a final temperature 25 °C (mixing ratio 1:15). (A) shows the mixing fraction of seawater into the hydrothermal fluid. (B) shows the concentrations of aqueous H_2S, H_2 and SO_4^{2-} and the pH (right-hand axis) as a function of temperature. (C) shows the concentration of aqueous Au species. The black-dashed lines correspond to the starting concentrations of Au and Ag in the modelled fluid from Table 2 of this electronic suppementary material (ESM 2); the grey-dotted line correspond to the maximum solubility over the reaction path. (D) shows the minerals that precipitate with mixing. No gold and silver precipitates under the modelled conditions. The apparent decrease in the amount of minerals precipitated at low temperature is an artifact of the increasing mass of fluid in the model as a result of mixing. Note: Because there is no information available about the As concentrations in this vent fluid, the formation of tennantite-(Fe, Zn) minerals cannot be considered in this model.

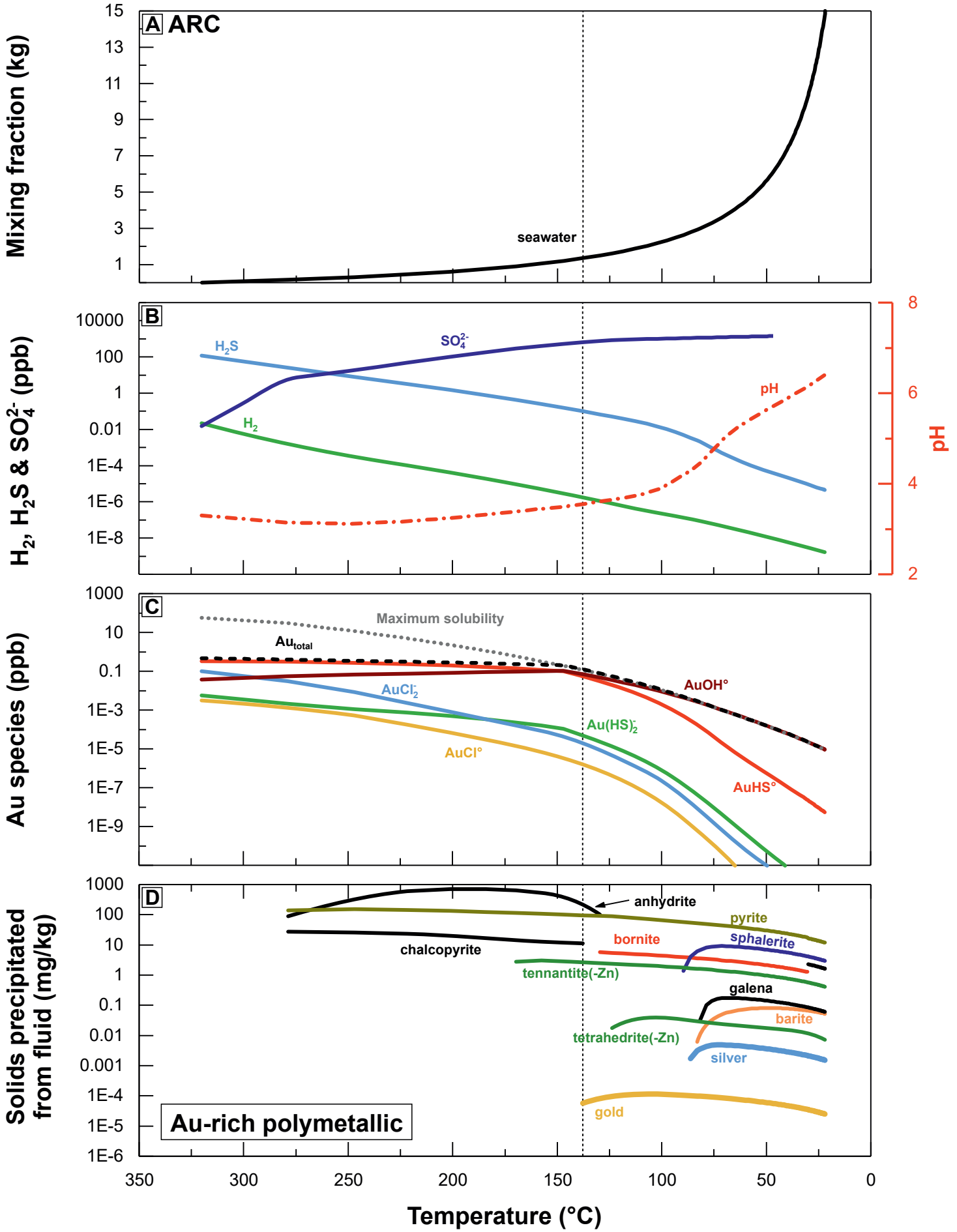

Fig. 4 (ESM 2) Geochemical reaction-path model for mixing of a typical arc-related (ARC) vent fluid with ambient seawater, using the starting composition of the Rogers Ruins field fluid samples (Table 2 in ESM 2). This model assumes incremental mixing with cold seawater (2 °C) until a final temperature 25 °C (mixing ratio 1:15). (A) shows the mixing fraction of seawater into the hydrothermal fluid. (B) shows the concentrations of aqueous H_2S, H_2 and SO_4^{2-} and the pH (right-hand axis) as a function of temperature. (C) shows the concentration of aqueous Au species. The black-dashed lines correspond to the starting concentrations of Au and Ag in the modelled fluid from from Table 2 of this electronic suppementary material (ESM 2); the grey-dotted line correspond to the maximum solubility over the reaction path. (D) shows the minerals that precipitate with mixing and the resulting Au-rich polymetallic sulfide assemblage at low temperatures. The apparent decrease in the amount of minerals precipitated at low temperature is an artifact of the increasing mass of fluid in the model as a result of mixing. Note: Because there is no information available about the Sb concentrations in this vent fluid, the formation of tetrahedrite-(Fe, Zn) minerals cannot be considered in this model.

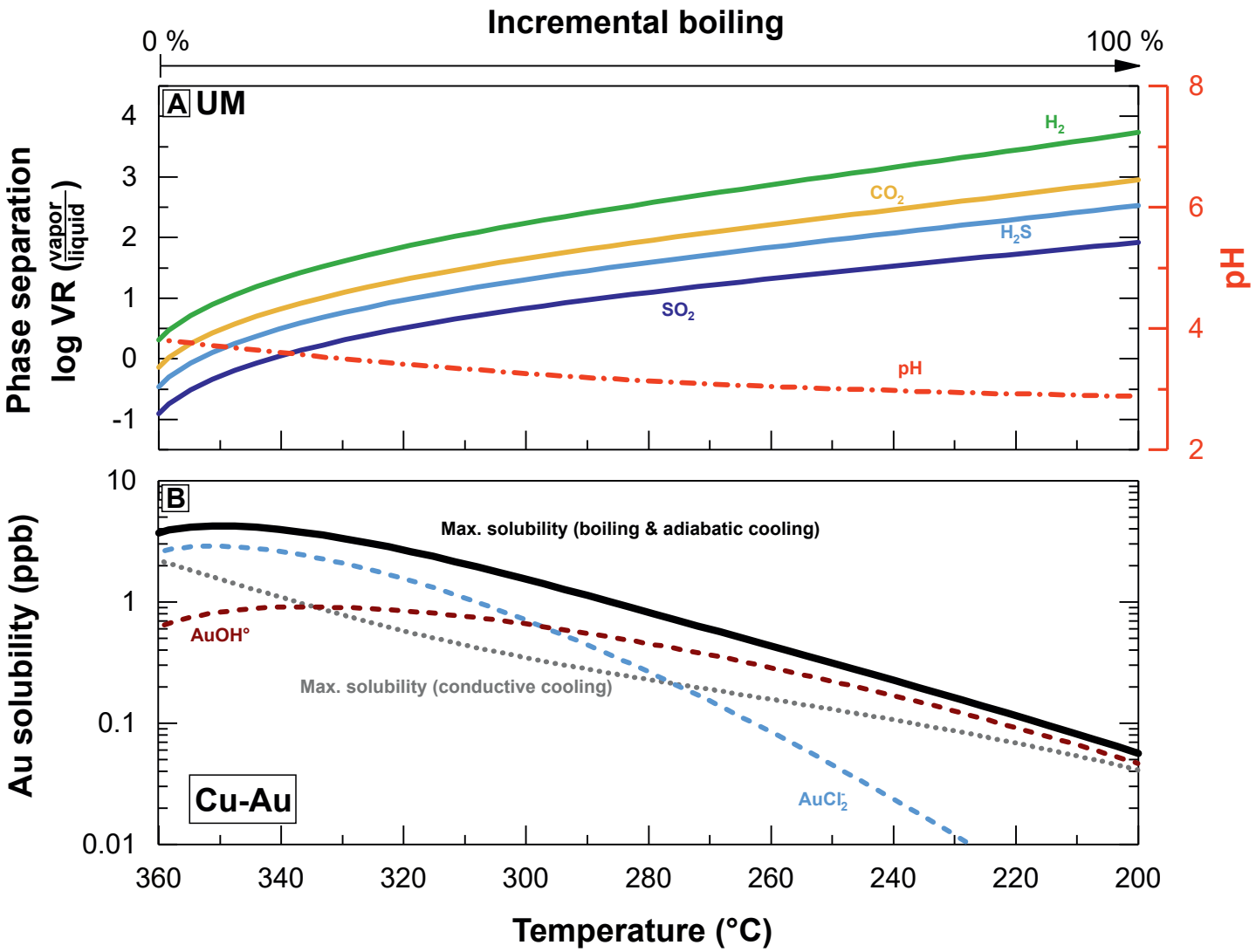

Fig. 5 (ESM 2) Model simulation of isoenthalpic boiling in an open system and associated adiabatic cooling of a typical ultramafic-hosted (UM) vent fluid (Table 2 in ESM 2) showing the maximum solubility gold. Boiling is simulated by combining the cooling model with the incremental loss of volatile gas species from 350 to 200°C following the method of Drummond and Ohmoto (1985). Gases are removed and the liquid re-equilibrated in a stepwise manner until 100% of the fluid has boiled at 200°C. (A) shows the partitioning of the volatile species, as well the pH (right axis). (B) shows the maximum solubility of gold (bold black line) during the boiling process as well as the predominant aqueous Au species (dashed lines). For comparison, the maximum solubility of Au from the corresponding conductive cooling model (see Fig. 11) is also plotted. The competing effects of H_2 and H_2S maintain a high solubility of gold over the entire reaction path, where the volatility of H_2 > H_2S and the fluids remain oxidized.

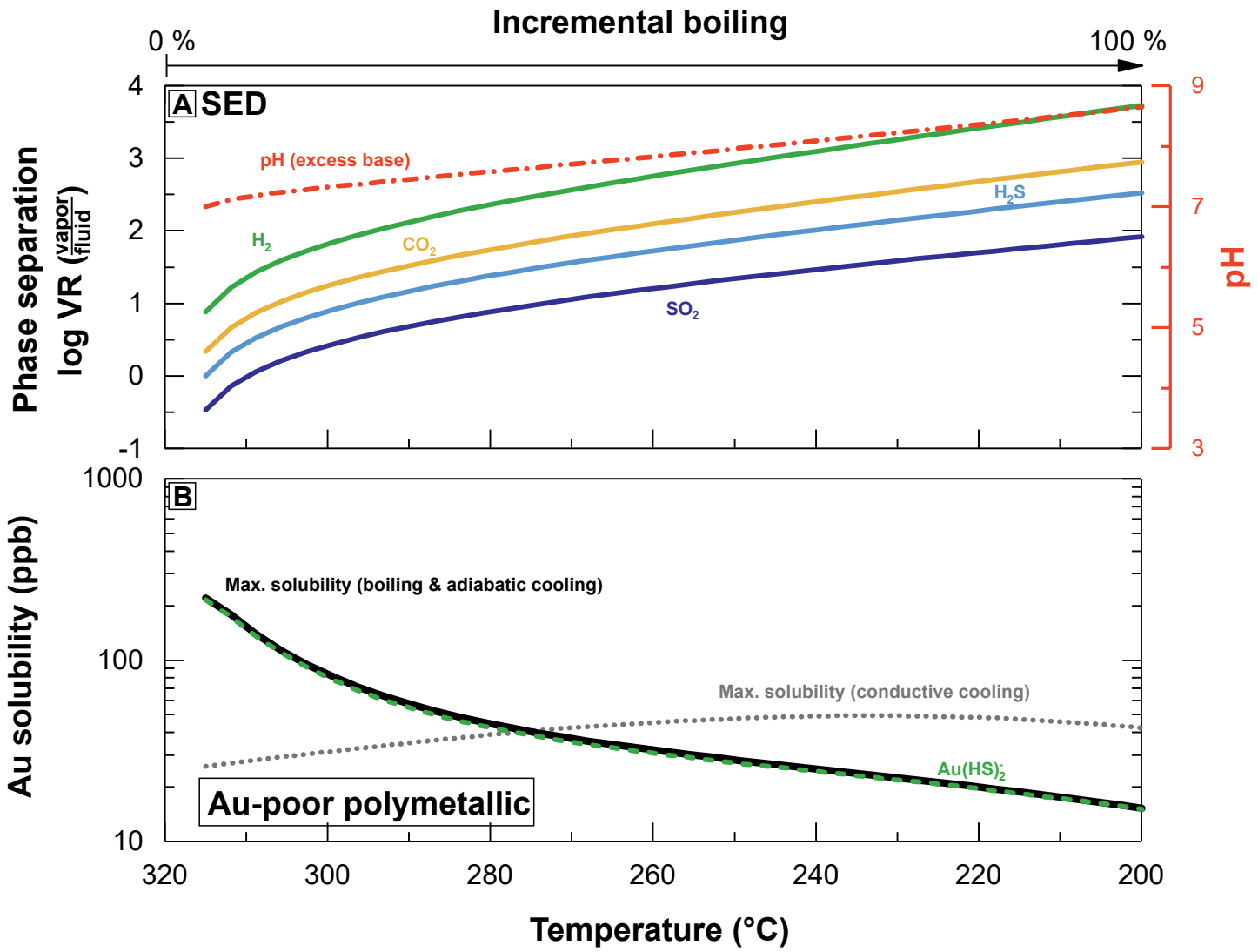

Fig. 6 (ESM 2) Model simulation of isoenthalpic boiling in an open system and associated adiabatic cooling of a typical sediment-hosted (SED) vent fluid (Table 2 in ESM 2) showing the maximum solubility gold. Boiling is simulated by combining the cooling model with the incremental loss of volatile gas species from 350 to 200°C following the method of Drummond and Ohmoto (1985). Gases are removed and the liquid re-equilibrated in a stepwise manner until 100% of the fluid has boiled at 200°C. (A) shows the partitioning of the volatile species, as well the pH (right axis). (B) shows the maximum solubility of gold (bold black line) during the boiling process as well as the predominant aqueous Au species (dashed lines). For comparison, the maximum solubility of Au from the corresponding conductive cooling model (see Fig. 12) is also plotted. The competing effects of H_2 and H_2S maintain a high solubility of gold until ~275°C , where the volatility of H_2 > H_2S and the fluids remain oxidized. The loss of H_2S eventually results in a decrease in the solubility of gold compared to the conductive cooling case (i.e., cross-over). Precipitation of gold under these conditions requires very high starting Au concentrations.

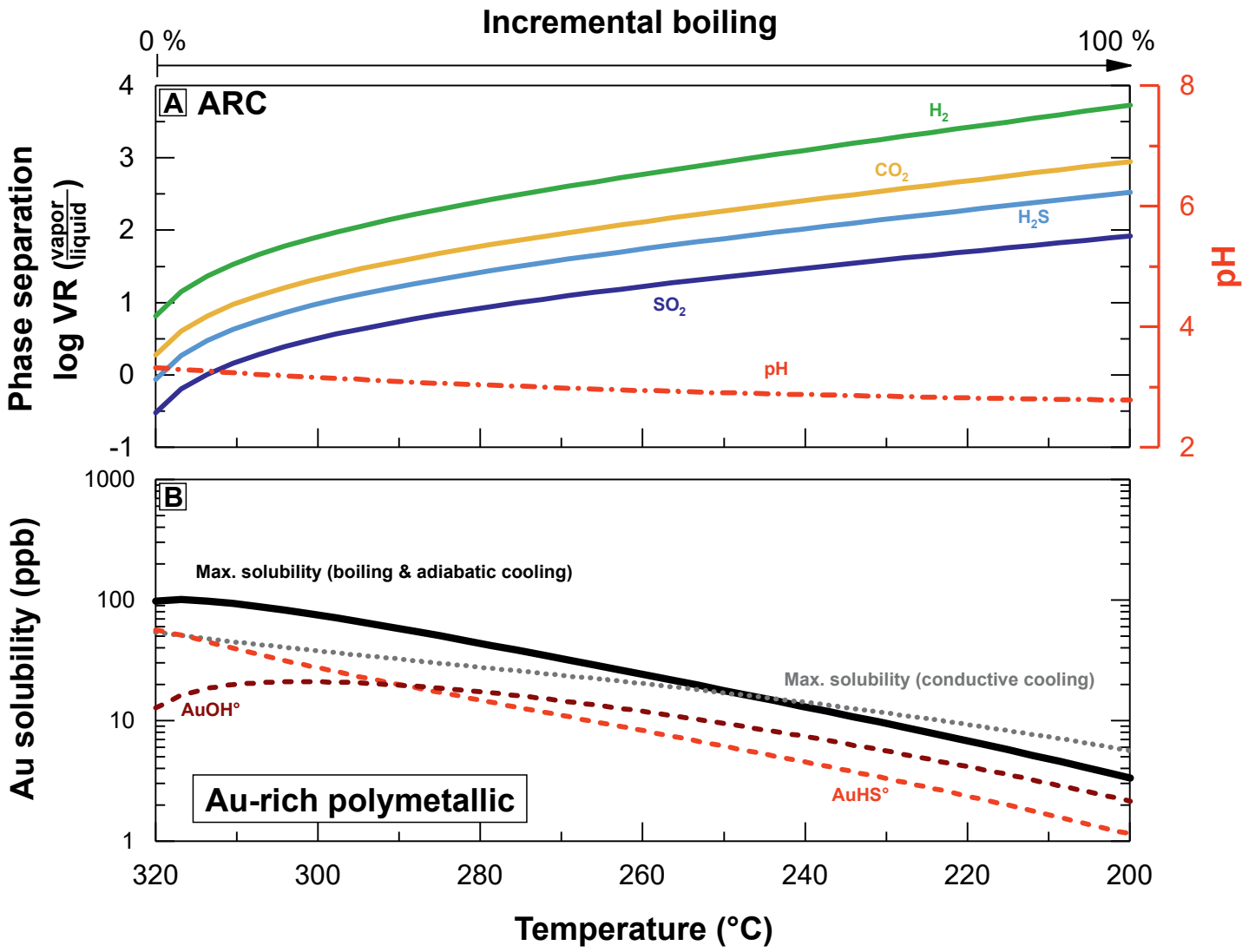

Fig. 7 (ESM 2) Model simulation of isoenthalpic boiling in an open system and associated adiabatic cooling of a typical arc-related (ARC) vent fluid (Table 2 in ESM 2) showing the maximum solubility gold. Boiling is simulated by combining the cooling model with the incremental loss of volatile gas species from 350 to 200 °C following the method of Drummond and Ohmoto (1985). Gases are removed and the liquid re-equilibrated in a stepwise manner until 100% of the fluid has boiled at 200 °C. (A) shows the partitioning of the volatile species, as well the pH (right axis). (B) shows the maximum solubility of gold (bold black line) during the boiling process as well as the predominant aqueous Au species (dashed lines). For comparison, the maximum solubility of Au from the corresponding conductive cooling model (see Fig. 13) is also plotted. The competing effects of H_2 and H_2S maintain a high solubility of gold until ~250 °C , where the volatility of H_2 > H_2S and the fluids remain oxidized. The loss of H_2S eventually results in a decrease in the solubility of gold compared to the conductive cooling case (i.e., cross-over). Precipitation of gold under these conditions requires very high starting Au concentrations.

Table 1 (ESM 2) List of aqueous and mineral species used in addition to the SUPCRT database

Species	References
Aqueous species	
$Ag(HS)^{\circ}$	Akinfiev and Zotov (2001)
$Ag(HS)_2^-$	Akinfiev and Zotov (2001)
$AgCl^{\circ}$	Akinfiev and Zotov (2001)
$AgCl_2^-$	Akinfiev and Zotov (2001)
AgOH	Akinfiev and Zotov (2001)
$Ag(OH)_2^-$	Akinfiev and Zotov (2001)
$Au(HS)^{\circ}$	Akinfiev and Zotov (2010)
$Au(HS)_2^-$	Akinfiev and Zotov (2010)
$AuCl^{\circ}$	Pokrovski et al. (2014)
$AuCl_2^-$	Pokrovski et al. (2014)
$AuOH^{\circ}$	Pokrovski et al. (2014)
$Au(OH)_2^-$	Pokrovski et al. (2014)
$Cu(HS)^{\circ}$	Akinfiev and Zotov (2010)
$Cu(HS)_2^-$	Akinfiev and Zotov (2010)
CuOH	Akinfiev and Zotov (2001)
$Cu(OH)_2^-$	Akinfiev and Zotov (2001)
$Zn(HS)_2^{\circ}$	Akinfiev and Tagirov (2012)
$Zn(HS)_3^-$	Akinfiev and Tagirov (2012)
$ZnCl_2^{\circ}$	Akinfiev and Tagirov (2012)
$ZnCl_3^-$	Akinfiev and Tagirov (2012)
$ZnCl_4^-$	Akinfiev and Tagirov (2012)
$Zn(OH)^+$	Akinfiev and Tagirov (2012)
$As(OH)_3^{\circ}$	Perfetti et al. (2008)
$AsO(OH)_3^{\circ}$	Perfetti et al. (2008)
Mineral species	
Tennantite-(Fe)	Seal et al. (1990)
Tennantite-(Zn)	Seal et al. (1990)
Tetrahedrite-(Fe)	Seal et al. (1990)
Tetrahedrite-(Zn)	Seal et al. (1990)
Arsenopyrite	Perfetti et al. (2008)

Table 2 (ESM 2) End-member composition of selected hydrothermal fluids and seawater used as input data for geochemical reaction-path modeling. The lower part of the table shows the activities and fugacities of the main species obtained by the speciation calculations.

Parameter (Unit)	Snakepit (MARK field)	Rainbow	Guaymas Basin	Rogers Ruins (PACMANUS)	Seawater
System Type	Basalt-hosted mid-ocean ridge (MORB)	Ultramafic rock-hosted mid-ocean ridge (UM)	Sediment-covered basalt-hosted mid-ocean ridge (SED-MORB)	Arc-rift related setting (ARC)	
	Input data for geochemical modeling				
T (°C)	341	362	315	320	2.00
Depth (m b.s.l.)	3500	2270	2000	1650 - 1780	
Pressure (bar)	352	228	201	166 - 179	
pH at 25°C	3.7	2.8	5.9	2.7	7.8
H_2S [mmol]	5.9	1.20	4.8	3.6	--
CO_2 [mmol]	6.7	16.0	61	7.3	2.30
H_2 [mmol]	0.48	16.0	3.4	0.02	$3x10^{-6}$
CH_4 [mmol]	0.062	2.50	63	0.032	$3x10^{-6}$
SO_4 [mmol]	--	--	--	--	28.0
Mg [mmol]	--	--	--	--	52
Cl [mmol]	550	750	599	648	540
Na [mmol]	515	533	485	488	464
K [mmol]	23.0	20.4	40	81	10.1
Ca [mmol]	11.0	67	34	27.1	10.2
Si [mmol]	20.0	7.1	13.8	18.8	0.1
Al [µmol]	12.0	1.90	6.5	6.7	0.02
Fe [mmol]	2.40	24.1	0.180	4.6	$5x10^{-4}$
Mn [µmol]	400	2250	139	2760	$3x10^{-4}$
Zn [µmol]	53	185	19.0	490	$5x10^{-3}$
Cu [µmol]	35	160	1.10	213	$3x10^{-3}$
Pb [µmol]	0.265	0.135	0.230	4.0	$1x10^{-5}$
Ba [µmol]	4.3	64	54	--	0.14
As [µmol]	0.231	--	1.07	17.1	$2.3x10^{-2}$
Sb [µmol]	0.011	0.003	--	0.32	$1.6x10^{-3}$
Au [nmol]	0.41[#]	0.41[#]	0.41[#]	2.00[$]	$1.52x10^{-4}$
Ag [nmol]	31	46	2.00	223	0.02
	Output speciation results - basis parameters				
pH (reservoir T, °C)	4.49	3.84	5.9*	3.32	
Gaseous species (log fugacity)					
H_2O	1.999	2.09	1.8739	1.90	
H_2	0.0108	0.5358	-0.065	-2.59	
O_2	-32.14	-31.61	-34.12	-28.64	
S_2	-11.74	-13.76	-12.34	-7.42	
H_2S	-0.79	-1.53	-0.84	-0.97	
CO_2	-0.40	-0.08	0.54	-0.31	
CH_4	-2.14	-0.67	1.04	-2.29	
SO_2	-11.08	-12.60	-11.98	-4.32	
Aqueous species (log activity)					
H_2	-2.24	-1.61	-2.44	-4.94	
H_2S	-2.22	-2.90	-2.32	-2.44	
HS^-	-5.63	-7.19	-4.03	-6.79	
CO_2	-2.16	-1.78	-1.34	-2.12	
CH_4	-4.19	-2.58	-1.18	-4.48	
Cl^-	-0.97	-1.01	-0.88	-0.86	
HCO_3^-	-6.69	-7.27	-4.07	-7.51	
OH^-	-6.83	-7.53	-5.34	-7.94	
$AuHS^\circ$	-9.48	-10.16	-10.31	-8.83	
$Au(HS)_2^-$	-10.95	-13.25	-10.14	-11.43	
$AuCl^\circ$	-12.38	-11.16	-15.20	-10.85	
$AuCl_2^-$	-11.75	-10.45	-14.61	-10.21	
$AuOH^\circ$	-10.38	-10.15	-11.40	-19.27	
$Au(OH)_2^-$	-18.73	-19.16	-18.34	-9.75	
$AgHS^\circ$	-9.43	-10.96	-9.11	-9.70	
$Ag(HS)_2^-$	-12.51	-15.59	-10.62	-13.96	
$AgCl^\circ$	-9.17	-8.96	-10.62	-8.38	
$AgCl_2^-$	-7.93	-7.81	-9.32	-7.04	
$Ag(OH)_2^-$	-21.65	-22.88	-20.17	-23.15	

Compositional data of the vent fluids has been compiled using the data from Von Damm (1990); Charlou et al. (2002); Douville et al. (2002); Von Damm (2005); Craddock (2009) and Reeves et al. (2011). Seawater compositions are taken from Li (1991); Bruland and Lohan (2004) and German and Damm (2004).

[#]Average Au concentrations are calculated using values from Campbell et al. (1987); Hall et al. (1988); Hannington and Scott (1989a); Falkner and Edmond (1990) and Hannington et al. (1991a).

*In situ pH is taken from Von Damm (1990).